Available online at www.sciencedirect.com
ScienceDirect
Trans. Nonferrous Met. Soc. China 23(2013) 377−384
Transactions of Nonferrous Metals Society of China
www.tnmsc.cn

Pipe reduction of miniature inner grooved copper tubes through rotary swaging process

Long-sheng LU[1], Yong TANG[1], Wei-qiang FANG[1], Jiang CHENG[2]

1. Key Laboratory of Surface Functional Structure Manufacturing of Guangdong High Education Institutes, South China University of Technology, Guangzhou 510640, China;
2. School of Chemistry and Chemical Engineering, South China University of Technology, Guangzhou 510640, China

Received 29 October 2011; accepted 12 March 2012

Abstract: A rotary swaging machine was applied to fabricating pipe reduction for miniature inner grooved copper tube (MIGCT) heat pipes. Compared with conventional swaging method, the axial feed of the designed rotary swaging machine was reached by a constant pushing force. The deformation of grooves in pipe reduced section during rotary swaging was analyzed. The shrinkage and extensibility of pipe reduction were measured and calculated. Furthermore, four aspects, including outer diameter, surface roughness, extensibility and processing time of pipe reduction, which were influenced by the pushing force, were considered. The results show that the tube wall thickness increases gradually along the *z*-axis at sinking section. However, the outer diameters, surface roughness and micro-cracks at reduced section tend to decrease along the *z*-axis. Besides, the effect of variation in the pushing force on the extensibility is limited while an increase in the pushing force results in a decrease of surface roughness. Therefore, a large pushing force within the limit is beneficial to pipe reduction manufacturing during rotary swaging process.

Key words: rotary swaging; radial forging; stepped tube; pipe reduction; inner grooved tube; tube sinking; pushing force; surface roughness

1 Introduction

Heat pipes are widely used for thermal control in electronic products, such as CPUs, LEDs and solar collectors. Generally, the miniature inner grooved copper tube (MIGCT) heat pipe is one of the most attractive types [1]. For the convenience of embedded fins, a sinking section at the head of a heat pipe is necessary during manufacturing [2]. Moreover, an extra long pipe reduced section is required for heat pipe sealing. Therefore, a stepped tube with a long length reduced section is necessary for heat pipe production. However, the pipe reduction manufacturing technology for heat pipe production is seldom reported. Because of low rigidity and weak strength, the raw material MIGCT for heat pipes is fragile during pipe reduction manufacturing. To avoid damage, incremental forming technologies are useful for applying.

Incremental process creates deformation within regions of the workpiece, and its main advantage lies in the low deformation load, which makes it able to manufacture thin-walled tube products [3]. Among the many incremental forming technologies, the ball spinning, radial forging and rotary swaging processes have potentials to apply in pipe reduction manufacturing from MIGCT.

Ball spinning has been widely applied in air-conditioner industry and widely studied [4]. However, as the wall thicknesses at sinking section and reduced section are being reduced after the ball spinning process [5], they will result in the shell strength reduction, which is critical to the quality of heat pipes.

Radial forging is a hot or cold forging process. With two or four forging dies, a large number of short strokes enable the workpiece to deform extensively. Due to the opposite motion of the hammers, the twist torque and axial force are relatively small. Hence, the radial forging

Foundation item: Project (U0834002) supported by the Key Program of NSFC−Guangdong Joint Funds of China; Projects (51005079, 20976055) supported by the National Natural Science Foundation of China; Project (10451064101005146) supported by the Natural Science Foundation of Guangdong Province, China; Project (20100172120001) supported by Specialized Research Fund for the Doctoral Program of Higher Education, China

Corresponding author: Long-sheng LU; Tel: +86-20-87114634; E-mail: meluls@scut.edu.cn

DOI: 10.1016/S1003-6326(13)62473-5

has advantages of smooth outer surface finish, less material usage, and minimum notch effect, etc. Conventionally, the radial forging was used for solid shaft production [6]. However, the radial forging has also been accepted for tubular product fabrication [7]. GHAEI et al [8] found that the cost, required load, energy and die wear rate were all reduced. However, the radial forging process used for tubes without mandrel mainly dealt with tubes without inner profile, and large diameter steel tubes [9].

Compared with radial forging, rotary swaging process has a relatively high frequency pulse stroking speed (1500 and 6000 strokes per minute) [10]. Therefore, the rotary swaging has higher deformation efficiency and productivity than that of radial forging. Since invented in 1960s, the rotary swaging has been widely used for rod and tube forming of different materials, such as pure magnesium [11], tool steels [12] and aluminum alloy 6060 [13]. LIM et al [14] and RONG et al [15] investigated the deformation characteristics of the tube product by the rotary swaging process. The results show that the dimensional precision and surface quality are affected by the axial feed and the reduction of diameter. Although the rotary swaging has also been applied to inner grooved tube manufacturing, it still needs an inside mandrel while processing.

In this work, a designed rotary swaging method without mandrel was applied to the MIGCT for pipe reduction manufacturing. To meet the requirements of heat pipes and study the procedure, the plastic deformation of MIGCT and the influence of the pushing force on product quality were discussed.

2 Experimental

2.1 Material

First, the raw material of MIGCT was fabricated from copper T2 by oil-filled high-speed spinning technology [16]. The outer diameter of MIGCT is 6 mm, the tube wall thickness is 194 μm, the teeth height is 266 μm, the teeth width is 169 μm, the grooves width is 133 μm, and the groove number is 55. Besides, the length of workpiece (L_0) is 240 mm. Before rotary swaging, further processing methods, including tempering and sizing, were used to keep the copper tubes straight. The yield strength ($\sigma_{0.2}$) and surface roughness of workpiece (R_a) are 68 MPa and 0.344 μm, respectively.

2.2 Apparatus

Based on the principle of rotary swaging, a machine used for producing MIGCT stepped tube was applied, as shown in Fig. 1(a). A push cylinder, whose working stroke is controlled by two travel switches, was used as feed unit. And the other designed details were described in Ref. [17].

In the rotary swaging machine, a swaging assembly driven by an AC motor, whose rotation speed is 560 r/min, is the main function unit. The swaging assembly mainly consists of 14 rollers, a roller retainer, a spindle, and two same groups of stamper and forging die, as shown in Fig. 1(b). The tool of swaging process is forging dies, which can be divided into four sections, including the guide, sinking, sizing and receding sections. The drawing angular of forging die is 13°, and the surface roughness on the sinking and sizing section of radial forging die (R_a) is 0.2 μm. In order to reduce the friction, copper plates are located at the interfaces between spindle and forging dies.

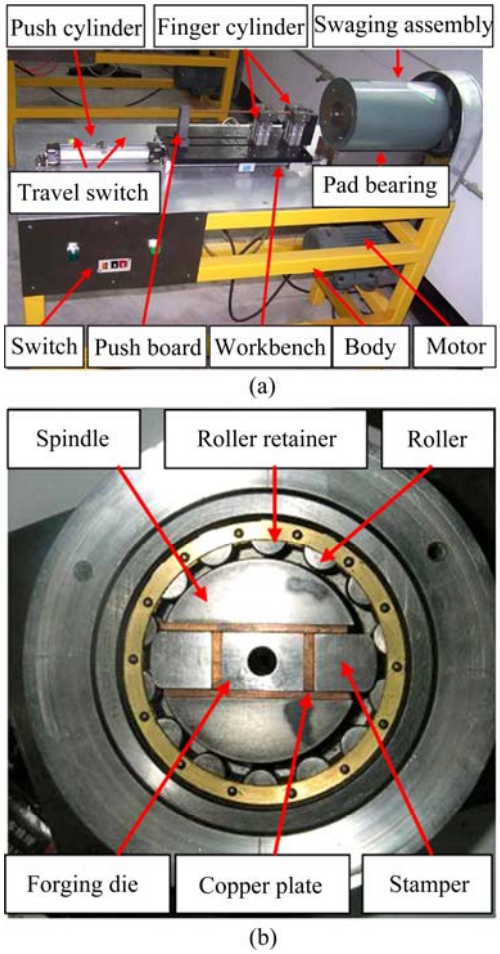

Fig. 1 Photos of rotary swaging machine (a) and swaging assembly (b)

2.3 Procedure

Firstly, a cylindrical MIGCT was prepared, and a push board was pulled to its start position by push cylinder. Secondly, a finger cylinder was opened getting ready for clamping workpiece. Thirdly, the workpiece of MIGCT was set into the holders, which will be driven by a finger cylinder to clamp MIGCT. A spindle was used to drive the forging dies. As the combination effect of AC

motor and rollers, 7840 short strokes per minute will act on the tube. Meanwhile, a push cylinder forced the MIGCT feeding at a constant pressure. After the push cylinder reached its end position, the feed of workpiece stopped, and then the push cylinder pulled the workbench back to its original position. The finger cylinder was consequentially released, and a stepped tube was fabricated. Figure 2 illustrates the schematic diagram of the stepped tube, where L_1 is the length of stepped tube, the length of sinking section (L_s) is 6mm and the length of reduced section (L_r) is 65mm. To evaluate the quality, the reduced section was divided into four sections continuously, in which the end points are named as *A*, *B*, *C*, *D* and *E*, respectively.

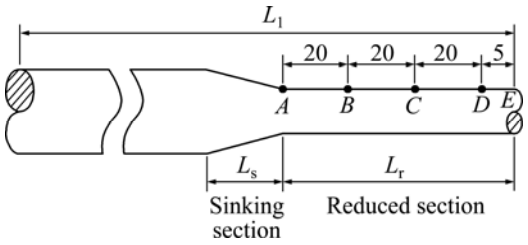

Fig. 2 Schematic diagram of stepped tube in axial (mm)

3 Results and analysis

3.1 Deformation

Compared with conventional radial forging or rotary swaging method, the workpiece in this study was MIGCT, which had a thin wall, long reduced section and numbers of grooves on the inner surface. Hence, the deformation mechanism of pipe reduced section should be investigated. All deformation tests in this section were conducted at a clamping force of 196.3 N and a pushing force of 321.7 N.

3.1.1 Groove deformation

Grooves are critical structures of MIGCT. The damaged or twisted grooves in the sinking section, especially in the original section, will result in the failure of recycling function of heat pipes. To explore the groove deformation during rotary swaging, a selected piece in axial cross section is illustrated in Fig. 3(a). The sample was chosen from the sinking section of the stepped tube. It is observed that the grooves disappear gradually along the *z*-axis in macroscopy, and the deformation of grooves mainly locates at the sinking section. Figure 3(b) shows

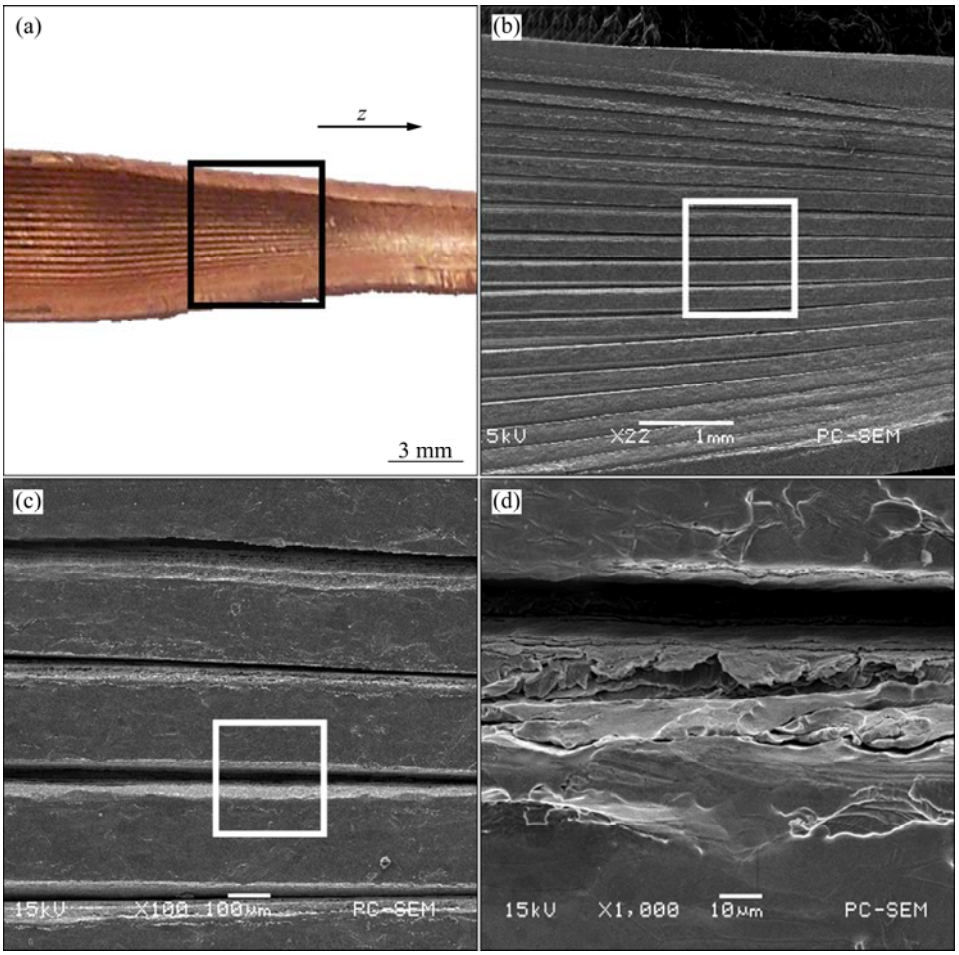

Fig. 3 SEM images of reduction in axial cross section: (a) Sample; (b) Partial enlarged view of (a); (c) Partial enlarged view of (b); (d) Groove image

that the groove width gradually decreases along the *z*-axis. Finally, the adjacent groove walls will extrude with each other, and only a tiny clearance leaves at the end of sinking section close to the reduced section. Meanwhile, the wall thickness of the tube also gradually increases along the *z*-axis, and the increments all happen at the sinking section. The decreasing trend of groove width can be observed more clearly in Fig. 3(c). Figure 3(d) reveals that the metal on the top of teeth is extrusive, while the metal on the bottom of teeth is sunk during swaging.

Figure 4(a) shows the SEM images of reduced section in radial cross section at sector *AB*. In the macroscopy view, it seems that the grooves totally disappear at the reduced section, and the tube wall thickness increases from 194 to 800 μm, but the hole diameter decreases from 5.08 mm (diameter of the top tooth circle) to 1.6 mm simultaneously. To make clear the deformation mechanism of tube wall, a partially enlarged SEM image, as shown in Fig. 4(b), was taken at the position close to the inner surface of reduced section, which reveals that small gaps between adjacent grooves still exist. Furthermore, Figure 4(c) illustrates that the size of gaps increases in reversed-radial direction due to a thin oxidized layer on the groove wall which leads to a non-uniform metallurgical structure. In this way, the cold welding stress of adjacent groove wall increases significantly. Furthermore, the compressive stress distribution during swaging decreases gradually in the reversed-radial direction in teeth, as indicated by TANG et al [18]. In this situation, cold welding of grooves will firstly occur at the bottom of the tooth. However, without a mandrel action during swaging, the compressive stress on the top of tooth can hardly reach the stress limitation of cold welding, so that tiny gaps still exist between grooves.

3.1.2 Outer surface deformation

The surface roughness and outer diameter distribution in axial direction is important to qualify heat pipes. Hence, the outer diameter was measured by a micrometer and the surface roughness was measured by a portable device (TR240). The sampling length in roughness measuring process was 0.8 mm. In order to reduce the random error, five measurements were done on different places randomly selected in the tested sector.

Figure 5 shows the surface roughness and outer diameter (d_o) distribution at reduced section in axial direction. The outer diameter of reduced section decreases from 3.296 mm at sector *AB* to 3.238 mm at sector *CD*, but remains the same from sector *CD* to sector *DE* at around 3.237 mm. Furthermore, the results indicate that the final outer diameter of reduced section is a little larger than that of the sizing section of forging dies whose diameter is limited as 3.22 mm. It may be

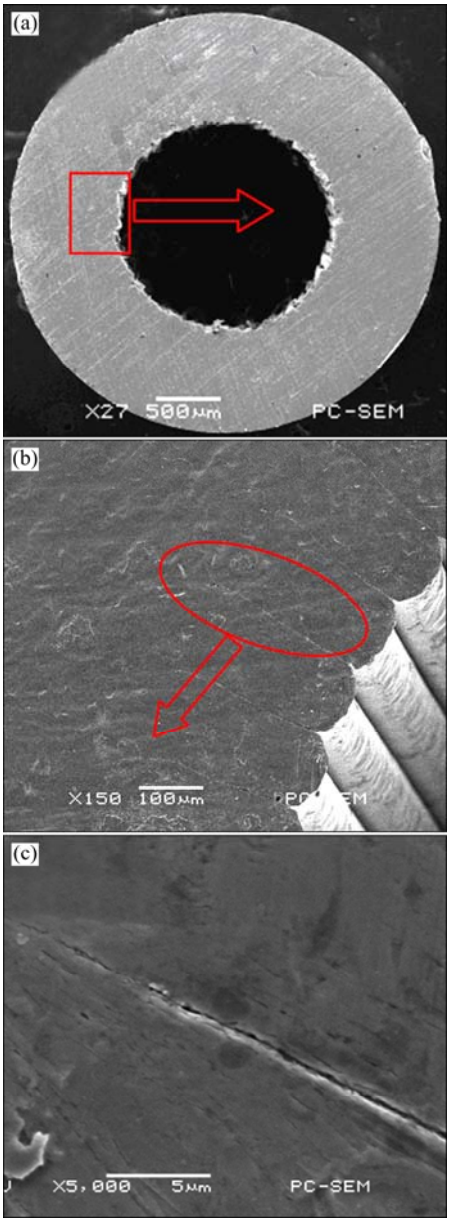

Fig. 4 SEM images of reduced section in cross section: (a) Sample; (b) Partial enlarged view of (a); (c) Gaps between each adjacent groove

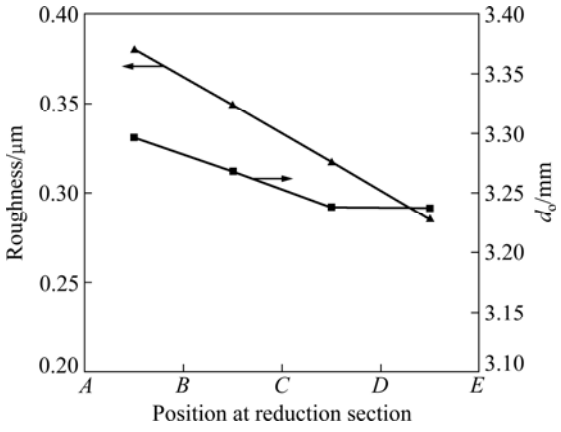

Fig. 5 Surface roughness and outer diameter distribution at reduced section in axial direction

caused by the rebound deformation of metal at the post-set time of each stroke during swaging. The results also show that the surface roughness at reduced section decreases linearly along the *z*-axis. At sector *AB*, the surface roughness is a litter larger than that of the workpiece. While at sector *DE*, the surface roughness reduced to 0.282 μm. The phenomena agree with the founding of LIM et al [14] very well.

Figure 6 shows the outer surface deformation behavior further. The surface of reduced section looks smooth from macroscopy. After enlarging 60 times, lots of micro-cracks, relatively parallel to the *z*-axis, emerge on the outer surface at reduced section. The dimensions of the micro-cracks are 1−3 μm in width, 5−10 μm in depth, and several millimeters in length. The distribution density of micro-cracks tends to decrease gradually along the *z*-axis which leads to improve the surface quality. During the swaging process, a large number of short strokes and high speed pressing operations were performed on the stepped tube by the forging dies. MIGCT was forced to sink until the post-set time of each stroke during swaging. A relative slide between the workpiece and forging dies in both axial and circumferential directions is small because of short post-set time. As a result, the plastic deformation traces generated by two nearby pressing operations emerge as micro-cracks. The sizes of micro-cracks will be reduced by the following numbers of pressing procedures along *z*-axis. So, the micro-cracks can be reduced by increasing the stroke number.

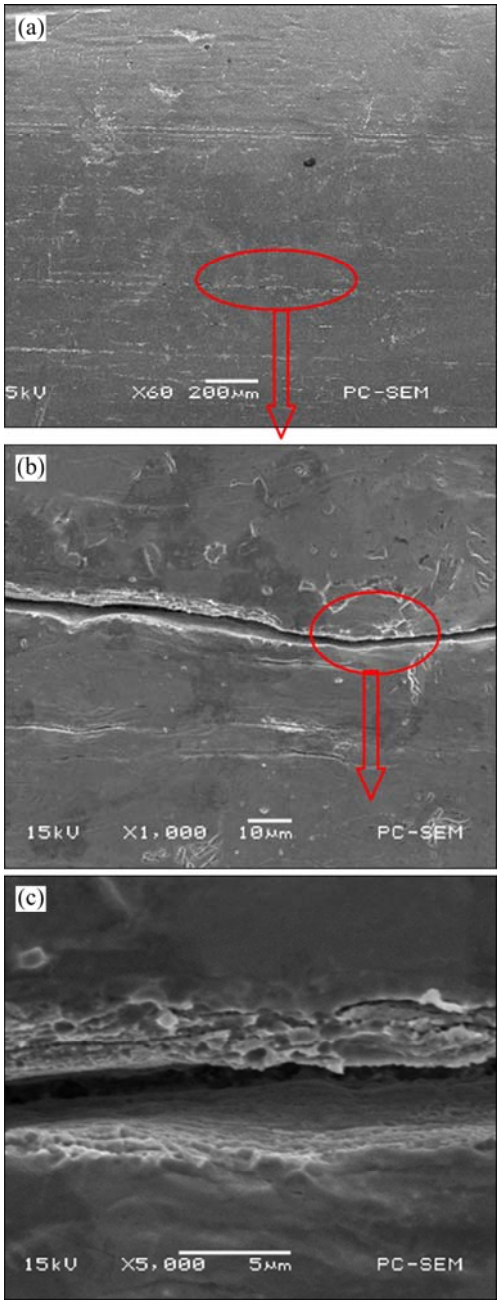

Fig. 6 SEM images of micro-cracks on outer surface at reduced section: (a) Sample; (b) Micro-cracks; (c) Partial enlarged view of (a)

3.1.3 Plastic deformation of pipe reduction

MIGCT will be elongated in axial direction and shrunk in radial cross section during rotary swaging. Based on the geometry of tube, the shrinkage ratio (ψ) at pipe reduced section, which can show the cross area change after swaging, can be calculated by the following formula:

$$\Psi=\left[1-\frac{\pi(d_{\mathrm{o}}^2-d_{\mathrm{i}}^2)/4}{2\pi R_0 t+nb_{\mathrm{t}}h}\right]\times 100\% \tag{1}$$

where d_{o} is the outer diameter of reduced section, and d_{i} is the inner diameter of reduced section; R_0 is the outer radius; t is the wall thickness; n is the groove number; b_{t} is the teeth width; h is the groove depth.

Substituting values of d_{o}=3.2 mm, d_{i}=1.6 mm, R_0=3 mm, t=0.194 mm, n=55, b_{t}=0.169 mm, h=0.266 mm into Eq. (1), we have ψ=1.59%.

In order to calculate the extensibility (δ) at the pipe reduced section, which illustrates the length change after swaging, two assumptions are made.

1) The tube wall thickness of sinking section increases linearly and δ at sinking section is only half of δ at reduced section.

2) The plastic deformation only occurs at pipe reduced section and sinking section. And the plastic deformation that might happen at the original section due to pushing force was neglected.

From the above two assumptions, the δ at pipe reduced section can be calculated from Eq. (2):

$$\frac{L_{\mathrm{s}}}{1+0.5\delta}+\frac{L_{\mathrm{r}}}{1+\delta}=L_0+L_{\mathrm{s}}+L_{\mathrm{r}}-L_1 \tag{2}$$

Substituting values of L_{s}=6 mm, L_{r}=65 mm, L_0=240 mm, L_1=74.06 mm, into Eq.(2), we have δ=24.24%.

Compared with the shrinkage ratio and extensibility at the pipe reduced section, the extensibility is larger than the shrinkage ratio during the rotary swaging.

3.2 Pushing force

LIM et al [14] discovered that the axial feed was the main parameter that affected the performance of rotary swaging. In this study, the axial feed was controlled by the pushing force. Therefore, a series of experiments were designed to evaluate the influences of pushing force on the deformation at pipe reduced section, including outer diameter, surface roughness, extensibility and processing time. To reduce the experimental error, each experiment was done three times, and the average value was recorded. A clamping force of 196.3 N and a pushing force ranging from 80.4 to 482.5 N were applied.

3.2.1 Outer diameter

Figure 7 illustrates the influence of pushing force on the outer diameter at reduced section. It shows that the outer diameter in sector *AB* decreases gradually, while no obvious decrease is observed in sectors *BC*, *CD* and *DE*. This may be due to a larger pushing force results in more intensive deformation in sinking section than that of small one, and the rebound deformation that mainly occurs at sector *BC* reduced. In general, the increment of pushing force is considered to be beneficial for improving the cylindricity at reduced section.

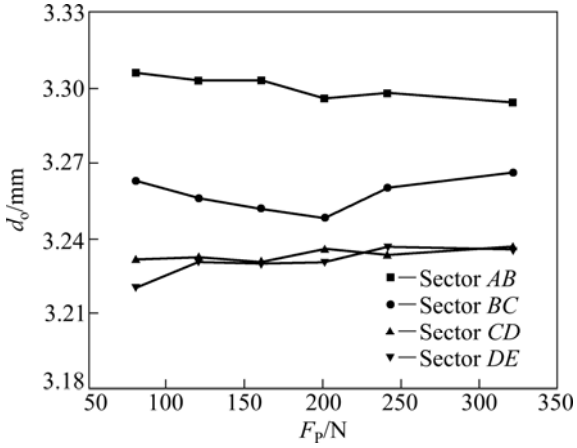

Fig. 7 Influence of pushing force (F_P) on outer diameter at reduced section

3.2.2 Surface roughness

Figure 8 shows the effect of pushing force on surface roughness at reduced section. Compared with conventional rotary swaging whose surface roughness normally decreases as the feeding speed increases, the surface roughness in all four sectors decreases as the pushing force increases. Furthermore, the largest decrease of roughness is found in sector *AB* and the smallest is in sector *DE*. And the differences of the roughness at reduced section decreases as the pushing force increases. All these phenomena can be explained by the relative rotation between the dies and workpiece [17]. Due to the friction force between the die-workpiece interfaces, the workpiece was observed rotating following the rotation of swaging dies. And the motion-opposing clamping force will result in the rotation speed of MIGCT smaller than the dies. Due to the high surface quality of the dies, the friction movement will decrease the surface roughness. A larger pushing force will bring a larger friction force, and the surface quality of pipe reduction will be improved. Therefore, a larger pushing force results in better surface roughness at reduced section. However, a further study of the relationship between pushing force and workpiece rotation needs to be done.

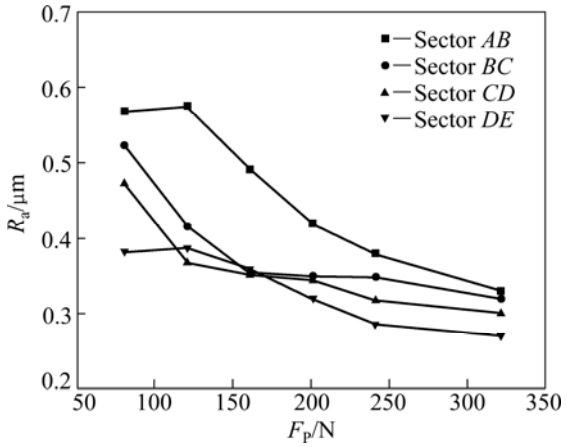

Fig. 8 Influence of pushing force on surface roughness

3.2.3 Extensibility

The extensibility at reduced section, however, remains almost constant as the pushing force increases, as shown in Fig. 9. It may be due to the fact that the extensibility is mainly influenced by the reduction ratio in diameter. But the detailed reason needs a further study. Therefore, the results suggest that the variations in pushing force yield insignificant effects on the

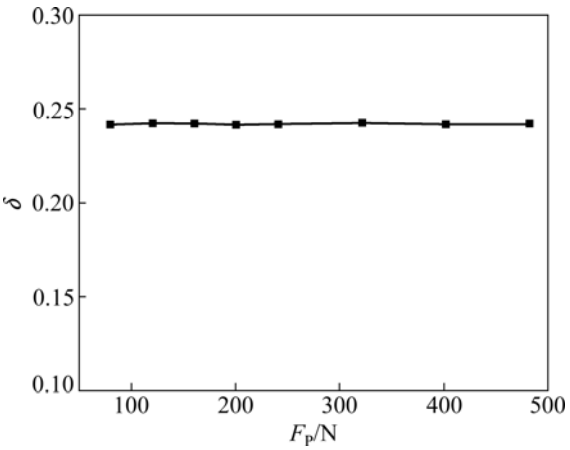

Fig. 9 Influence of pushing force on tube extensibility

extensibility at reduced section. In view of extensibility, the pushing force can be chosen at any extent.

3.2.4 Processing time

The processing time is defined as the time consumption to produce a stepped tube. The influence of pushing force on processing time is shown in Fig.10. It illustrates that an increase of the pushing force leads to a decrease of processing time. While the pushing force increases from 160.8 N to 402.1 N, the time consumption to produce a stepped tube decreases from 13.95 s to 6.83 s. With the further increment of pushing force, the processing time of stepped tube only decreases slightly. This can be used as an evidence of that the feeding rate does not simply linearly scale up with the pushing force. Generally, the results suggest that a large pushing force increases the productivity.

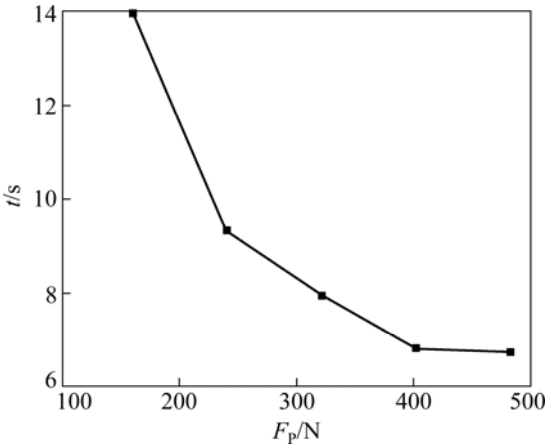

Fig. 10 Influence of pushing force on processing time (t)

3.2.5 Determination of pushing force

The influences of pushing force at reduced section on the outer diameter, surface roughness, extensibility and processing time are slightly different as investigated. The effect on the processing time is the greatest. Next to the processing time, the pushing force also has a major influence on the surface roughness, yet yields little or no effect on the extensibility. Although the results imply that a large pushing force is beneficial to pipe reduction processing, there are some factors limiting the pushing force, i.e., the rotation of spindle, the machine power, the friction at the interface between forging dies and workpiece, technological properties and strength of workpiece. With the selected operational parameters, i.e., the clamping force 196.3 N and the pushing force 321.7 N, the MIGCT can be forged into stepped tubes with long length reduced section effectively and economically.

4 Conclusions

1) During rotary swaging, the groove width decreases and tube wall thickness increases gradually along the z-axis at sinking section. However, small gaps between adjacent grooves appear, and their sizes increase in reverse-radial direction.

2) The outer diameters, surface roughness and micro-cracks at reduced section tend to decrease along the z-axis. Owing to the rebound deformation of metal at the post-set time of each stroke, the final outer diameter of reduced section is slightly larger than that of the sizing section of forging dies.

3) The extensibility at pipe reduced section is much larger than the shrinkage ratio during swaging.

4) A large pushing force within the limit is beneficial to pipe reduction manufacturing during rotary swaging process.

Acknowledgement

The authors would like to give our sincere thanks to Qin LU and Wei YUAN for their detailed modifications on the English writing of this paper.

References

[1] LU Long-sheng, TANG Yong, YUAN Dong, JIANG Le-lun. Micro heat pipe manufacturing technology of vacuuming and filling work fluid [J]. Journal of Mechanical Engineering, 2009, 45(6): 122−127. (in Chinese)

[2] WANG J C, HUANG H S, CHEN S L. Experimental investigations of thermal resistance of a heat sink with horizontal embedded heat pipes [J]. International Communications in Heat and Mass Transfer, 2007, 34(8): 958−970.

[3] GROCHE P, FRITSCHE D, TEKKAYA E A, ALLWOOD J M, HIRT G, NEUGEBAUER R. Incremental bulk metal forming [J]. CIRP Annals−Manufacturing Technology, 2007, 56(2): 635−656.

[4] LI Yong, XIAO Hui. Forming method of axial micro grooves inside copper heat pipe [J]. Transactions of Nonferrous Metals Society of China, 2008, 18(2): 1229−1212.

[5] PRAKASH R, SINGHAL R P. Shear spinning technology for manufacture tubes of small bore of long thin wall [J]. Journal of Materials Processing Technology, 1995, 54(1−4): 186−192.

[6] SAHOO A K, TIWARI M K, MILEHAM A R. Six sigma based approach to optimize radial forging operation variables [J]. Journal of Materials Processing Technology, 2008, 202(1−3): 125−136.

[7] GHAEI A, TAHERI A K, MOVAHHEDY M R. A new upper bound solution for analysis of the radial forging process [J]. International Journal of Mechanical Sciences, 2006, 48(11): 1264−1272.

[8] GHAEI A, MOVAHHEDY M R, KARIMI TAHERI A. Finite element modelling simulation of radial forging of tubes without mandrel [J]. Materials and Design, 2008, 29(4): 867−872.

[9] DOMBLESKY J P, SHIVPURI R, PAINTER B. Application of the finite-element method to the radial forging of large diameter tubes [J]. Journal of Materials Processing Technology, 1995, 49(1−2): 57−74.

[10] RONG Long, NIE Zuo-ren, ZUO Tie-yong. 3D finite element modeling of cogging-down rotary swaging of pure magnesium square billet—Revealing the effect of high-frequency pulse stroking [J]. Materials Science and Engineering A, 2007, 464(1−2): 28−37.

[11] RONG Li, NIE Zuo-ren, ZUO Tie-yon. FEA modeling of effect of axial feeding velocity on strain field of rotary swaging process of pure magnesium [J]. Transactions of Nonferrous Metals Society of China, 2006, 16(5): 1015−1020

[12] GROSMAN F, PIELA A. Metal flow in the deformation gap at primary swaging [J]. Journal of Materials Processing Technology, 1996, 56(1−4): 404−411.
[13] GROCHE P, TURK M. Smart structures assembly through incremental forming [J]. CIRP Annals−Manufacturing Technology, 2011, 60(1): 21−24.
[14] LIM S J, CHOI H J, LEE C H. Forming characteristics of tubular product through the rotary swaging process [J]. Journal of Materials Processing Technology, 2009, 209(1): 283−288.
[15] RONG Li, NIE Zuo-ren, ZUO Tie-yong. Effects of reduction of diameter on microstructure and surface roughness of rotary swaged magnesium by FEA [J]. Transactions of Nonferrous Metals Society of China, 2008, 18(s1): 263−268.
[16] TANG Yong, CHI Yong, CHEN Jin-cang, DENG Xue-xiong, LIU Lin, LIU Xiao-kang, WANG Zhen-ping. Experimental study of oil-filled high-speed spin forming micro-groove fin-inside tubes [J]. International Journal of Machine Tools and Manufacture, 2007, 47(7−8): 1059−1068.
[17] LU Long-sheng, YUAN Dong, TANG Yong, CHENG Jiang. Slave rotation analysis of miniature inner grooved copper tube through rotary swaging process [J]. The International Journal of Advanced Manufacturing Technology, 2011, 61(1−4): 185−193.
[18] TANG Yong, LU Long-sheng, YUAN Dong, WANG Qing-hui, ZHAO Xiao-lin. Experimental and FEM study on sinking of miniature inner grooved copper tube [J]. Journal of Materials Processing Technology, 2009, 209(12−13): 5333−5340.

细小内沟槽铜管的回转模锻管端缩径

陆龙生[1]，汤 勇[1]，方伟强[1]，程 江[2]

1. 华南理工大学 表面功能结构先进制造广东普通高校重点实验室，广州 510640；
2. 华南理工大学 化学与华工学院，广州 510640

摘 要：为制造小型沟槽铜热管，设计和采用了回转模锻工艺进行管端缩径。相比传统的回转模锻，所使用的回转模锻机的轴向进给通过恒定的推力实现。采用实验方法，分析旋转模锻过程中缩径段的沟槽变形，测量和计算管端缩径过程的截面收缩率和伸长率。探讨进给推力对缩径段的直径、表面粗糙度、伸长率和加工时间的影响。结果表明：缩径段的管壁厚度沿着轴向逐渐增长，而外径、表面粗糙度和微观裂纹则沿轴向逐渐减小。此外，推力对伸长率的影响很小，而表面粗糙度则随着推力的增大而减小。因此，采用回转模锻进行管端缩径，在允许范围内，增大进给推力对管端缩径质量有益。

关键词：回转模锻；径向锻造；阶梯管；管端缩径；内沟槽管；缩管；进给推力；表面粗糙度

(Edited by Xiang-qun LI)